NUCL SCI TECH (2018) 29:177
https://doi.org/10.1007/s41365-018-0510-1

Collective flow and nuclear stopping in heavy ion collisions in Fermi energy domain

Peng-Cheng Li[1,2] · Yong-Jia Wang[2] · Qing-Feng Li[2,3] · Hong-Fei Zhang[1,3]

Received: 31 August 2018 / Revised: 8 October 2018 / Accepted: 9 October 2018 / Published online: 17 November 2018

Abstract The effects of the in-medium nucleon–nucleon (NN) elastic cross section on the observables in heavy ion collisions in the Fermi energy domain are investigated within the framework of the ultrarelativistic quantum molecular dynamics model. The results simulated using medium correction factors of $\mathcal{F} = \sigma_{\mathrm{NN}}^{\mathrm{in-medium}}/\sigma_{\mathrm{NN}}^{\mathrm{free}} = 0.2, 0.3, 0.5$, and the density- and momentum-dependent factor obtained from the FU3FP1 parametrization are compared with the FOPI and INDRA experimental data. It is found that the calculations using the correction factors $\mathcal{F} = 0.2$ and 0.5 reproduce the experimental data (i.e., collective flow and nuclear stopping) at 40 and 150 MeV/nucleon, respectively. Calculations with the FU3FP1 parametrization can best fit these experimental data. These conclusions can be confirmed in both $^{197}\mathrm{Au} + ^{197}\mathrm{Au}$ and $^{129}\mathrm{Xe} + ^{120}\mathrm{Sn}$.

This work was supported by the National Natural Science Foundation of China (Nos. 11875125, 11747312, 11675066, and 11505057) and the Zhejiang Provincial Natural Science Foundation of China (No. LY18A050002).

✉ Yong-Jia Wang
wangyongjia@zjhu.edu.cn

✉ Qing-Feng Li
liqf@zjhu.edu.cn

[1] School of Nuclear Science and Technology, Lanzhou University, Lanzhou 730000, China

[2] School of Science, Huzhou University, Huzhou 313000, China

[3] Institute of Modern Physics, Chinese Academy of Sciences, Lanzhou 730000, China

Keywords Nucleon–nucleon elastic cross section · Heavy ion collisions · Nuclear stopping · Collective flow

1 Introduction

The properties of hot, dense nuclear matter are usually extracted by comparing the observables in heavy ion collision (HIC) experiments with the corresponding results from transport model simulations. The most popular transport methods for studying HICs at low and intermediate energies are the quantum molecular dynamics (QMD) model [1], the Boltzmann (Vlasov)–Uehling–Uhlenbeck (BUU or VUU) model [2], and their improved versions [3–5]. The mean-field potential and nucleon–nucleon cross section (NNCS) are two essential components of these models. The mean-field potential in transport models has been studied extensively [6–8]. Regarding the NNCS, it is well known that compared with the free NNCS, the in-medium NNCS is suppressed [9–26]; however, the degree of suppression is still uncertain and requires further improvement. Thus, the in-medium NNCS has been studied by many groups using different methods [27–41].

Recently, a systematic experimental study of nuclear stopping in central collisions at intermediate energies pointed out that the correction factor $\mathcal{F} = \sigma_{\mathrm{NN}}^{\mathrm{in-medium}}/\sigma_{\mathrm{NN}}^{\mathrm{free}}$ is deduced to be 0.16 ± 0.04 at 40 MeV/nucleon and 0.5 ± 0.06 at 100 MeV/nucleon [42]. New opportunities emerged to study the in-medium NNCS using transport models based on these stopping data [43–46]. There are many parameterized in-medium NNCSs adopted by various models. For example, $\sigma_{\mathrm{NN}}^{\mathrm{in-medium}} = (1 - \eta\rho/\rho_0)\sigma_{\mathrm{NN}}^{\mathrm{free}}$ with $\eta = 0.2$ has been adopted in the BUU, relativistic BUU, and improved QMD models [10, 19, 20]. In the pBUU

model, the in-medium NNCS is independent of the density, energy, and isospin and reads as $\sigma_{\rm NN}^{\rm in-medium} = 0.85\rho^{-2/3}/\tanh\left(\frac{\sigma^{\rm free}}{0.85\rho^{-2/3}}\right)$ [23]. In the isospin-dependent BUU model and the Lanzhou QMD model [47], the NNCS in the nuclear medium is corrected by a factor of $\mathcal{F} = \sigma_{\rm NN}^{\rm in-medium}/\sigma_{\rm NN}^{\rm free} = (\mu_{\rm NN}^{*}/\mu_{\rm NN})^2$. Here, $\mu_{\rm NN}$ and $\mu_{\rm NN}^{*}$ are the k masses of the colliding nucleon partners in free space and in the nuclear medium, respectively [16, 17, 24, 48]. In our previous works, we found that the collective flow and nuclear stopping can be reproduced using the parameterized medium correction factor $\mathcal{F}$ (which depends on the density and momentum) for the free NNCS within the ultrarelativistic QMD (UrQMD) model [49–53]. It is desirable to evaluate the differences between the $\mathcal{F}$ values extracted from experimental data [42] and the parameterized one adopted currently in the UrQMD model.

This paper is organized as follows. In Sect. 2, we review the UrQMD model with the improved potential. Section 3 presents an investigation of the effects of the in-medium NNCS on the observables of free protons and hydrogen isotopes in HICs in the Fermi energy domain. Finally, a summary is given in Sect. 4.

2 Model description and observables

The UrQMD model is based on the same principles as the QMD model. In the UrQMD model, more than 55 different baryon and 32 different meson species, as well as the corresponding antiparticle and isospin-projected states, are considered. The model has been extensively and successfully used to study the nuclear reactions of $p + p$, $p +$ A, and A + A systems within a large range of beam energies, from the low-energy regime of the INDRA/GSI experiments up to the highest energies presently available at LHC/CERN. In addition, the other two main features unique to the collision term of the UrQMD model are the unique collision time for each individual collision and the two-step particle production process. More discussions can be found in recent works on the transport model comparison project, i.e., Refs. [3, 4].

At intermediate energies, the potential used in the UrQMD model depends on the momentum and density [1, 49, 54] and reads as

$$U = \alpha\cdot\left(\frac{\rho}{\rho_0}\right) + \beta\cdot\left(\frac{\rho}{\rho_0}\right)^{\gamma} + t_{\rm md}\ln^2\left[1 + a_{\rm md}(\mathbf{p}_i - \mathbf{p}_j)^2\right]\frac{\rho}{\rho_0}. \tag{1}$$

Here, $\alpha = -393$ MeV, $\beta = 320$ MeV, $\gamma = 1.14$, $t_{\rm md} = 1.57$ MeV, and $a_{\rm md} = 0.0005$ MeV^{-2}; these values yield an incompressibility K_0 of 200 MeV for isospin-symmetric nuclear matter. In order to better describe the recent experimental data, the surface, surface asymmetry energy, and symmetry energy terms obtained from the Skyrme potential energy density functional have been further introduced into the present version [51–53, 55, 56]:

$$\begin{aligned} u_{\rm Skyrme} =& u_{\rm sur} + u_{\rm sur,iso} + u_{\rm sym} \\ =& \frac{g_{\rm sur}}{2\rho_0}(\nabla\rho)^2 + \frac{g_{\rm sur,iso}}{2\rho_0}[\nabla(\rho_{\rm n} - \rho_{\rm p})]^2 \\ &+ \left(A_{\rm sym}\frac{\rho^2}{\rho_0} + B_{\rm sym}\frac{\rho^{\eta+1}}{\rho_0^{\eta}} + C_{\rm sym}\frac{\rho^{8/3}}{\rho_0^{5/3}}\right)\delta^2. \end{aligned} \tag{2}$$

$$\frac{gsur}{2} = \frac{1}{64}(9t_1 - 5t_2 - 4x_2t_2)\rho_0, \tag{3}$$

$$\frac{gsur,iso}{2} = -\frac{1}{64}[3t_1(2x_1 + 1) + t_2(2x_2 + 1)]\rho_0, \tag{4}$$

$$A_{\rm sym} = -\frac{t_0}{4}(x_0 + 1/2)\rho_0, \tag{5}$$

$$B_{\rm sym} = -\frac{t_3}{24}(x_3 + 1/2)\rho_0^{\eta}, \tag{6}$$

$$C_{\rm sym} = \frac{1}{24}\left(\frac{3\pi^2}{2}\right)^{2/3}\rho_0^{5/3}\Theta_{\rm sym}, \tag{7}$$

where $\Theta_{\rm sym} = 3t_1x_1 - t_2(4 + 5x_2)$ [51–53]. In this work, the SV-sym34 force, which gives $g_{\rm sur} = 18.2$ MeV fm^2, $g_{\rm sur,iso} = 8.9$ MeV fm^2, $A_{\rm sym} = 20.3$ MeV, $B_{\rm sym} = 14.4$ MeV, $C_{\rm sym} = -9.2$ MeV, and the slope parameter of the symmetry energy $L = 80.95$ MeV, is chosen.

In the UrQMD model, the in-medium NN elastic cross section is the product of the free cross sections with a medium correction factor $\mathcal{F}(\rho, p)$, which is momentum and density dependent. In the UrQMD model, the free proton-neutron cross sections are larger than the free neutron-neutron (proton-proton) cross sections at low beam energy, which is consistent with experimental data. In our previous work [18, 38–40, 50], we found that the medium correction factor F depends on the density, momentum, and isospin. However, the isospin dependence is relatively weak, see, e.g., [57, 58].

$$\sigma_{\rm NN}^{\rm in-medium} = \mathcal{F}(\rho, p) * \sigma_{\rm NN}^{\rm free}, \tag{8}$$

$$\mathcal{F}(\rho, p) = \frac{\lambda + (1 - \lambda)e^{-\rho/\rho_0/\zeta} - f_0}{1 + (p_{\rm NN}/p_0)^{\kappa}} + f_0. \tag{9}$$

Here, $\lambda = 1/3$, $\zeta = 1/3$, $f_0 = 1$, $p_0 = 0.425$ GeV/c, and $\kappa = 5$, which corresponds to the FU3FP1 parametrization used in Ref. [50]. Moreover, $\mathcal{F}(\rho, p)$ is set to unity when $p_{\rm NN}$ is larger than 1 GeV/c.

The in-medium correction factor $\mathcal{F}(\rho, p)$ obtained from the FU3FP1 parametrization as functions of both the reduced density ρ/ρ_0 and momentum $p = p_{\rm NN}$ is shown in Fig. 1. It is seen that the values deduced from the

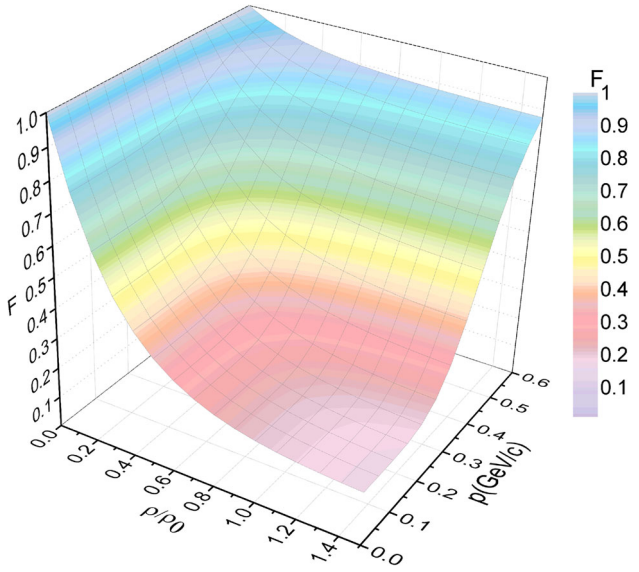

Fig. 1 (Color online) In-medium correction coefficient $\mathcal{F}$ obtained from the parametrization FU3FP1, which is density and momentum dependent

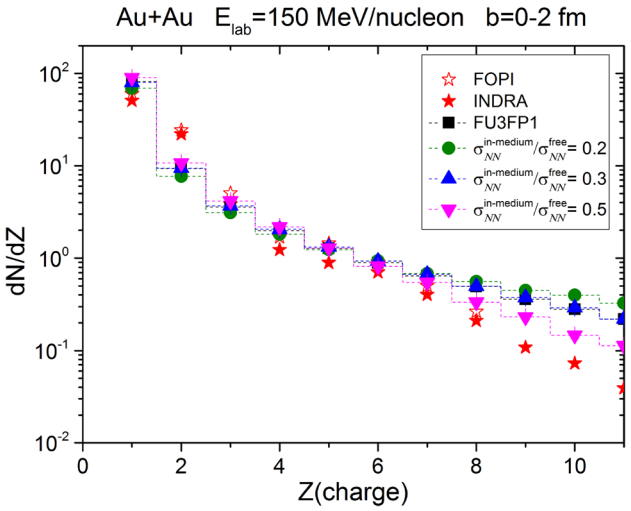

Fig. 2 (Color online) Charge multiplicity distribution in ^{197}Au + ^{197}Au central collisions at beam energy of 150 MeV/nucleon. The experimental data are taken from Ref. [69]. The calculations performed with the in-medium correction factors of $\mathcal{F} = 0.2$ (circles), $\mathcal{F} = 0.3$ (up-facing triangles), and $\mathcal{F} = 0.5$ (down-facing triangles) are compared with calculations using the FU3FP1 parametrization of the in-medium NNCS (squares)

experiment [42] can be covered by the values of the in-medium correction factor $\mathcal{F}(\rho, p)$ obtained from the FU3FP1 parametrization. In order to compare the effect of the in-medium NN cross section on the collective flow and nuclear stopping, three fixed values, $\mathcal{F} = 0.2$, 0.3, and 0.5, are further adopted in this work.

3 Results and discussion

3.1 Charge distribution

In this work, fragments are recognized by the isospin-dependent minimum spanning tree (iso-MST) method. Nucleons with relative distances smaller than $R_0^{\mathrm{pp}} = 2.8$ fm, $R_0^{\mathrm{nn}} = R_0^{\mathrm{np}} = 3.8$ fm and relative momenta smaller than $P_0 = 0.25$ GeV/c are considered to belong to the same cluster. The charge distribution of Au + Au collisions at a beam energy of 150 MeV/nucleon is displayed in Fig. 2. The distribution of charged fragments decreased exponentially with increasing charge number, and this behavior can be reproduced by both the simulations with FU3FP1 and those with the fixed in-medium correction factors. For large fragments ($Z \geq 6$), calculations with $\mathcal{F} = 0.5$ seem to be closer to the experimental data. However, one cannot conclude that $\mathcal{F} = 0.5$ is preferable to the others because the charge distribution will also be affected by unconstrained (or less constrained) parameters in the transport model; for example, the chosen coalescence model parameters will strongly influence the charge distribution but not the collective flow and nuclear stopping [51–53, 59–68].

3.2 Collective flow

One can obtain the directed (v_1) and elliptic (v_2) flows from the Fourier expansion of the azimuthal distribution of detected particles [70, 71]; they read as

$$v_1 \equiv \langle \cos(\phi) \rangle = \left\langle \frac{p_x}{p_{\mathrm{t}}} \right\rangle, \tag{10}$$

$$v_2 \equiv \langle \cos(2\phi) \rangle = \left\langle \frac{p_x^2 - p_y^2}{p_{\mathrm{t}}^2} \right\rangle, p_{\mathrm{t}} = \sqrt{p_x^2 + p_y^2}. \tag{11}$$

The reduced rapidity (y_z/y_{pro}) dependence of the directed (v_1) and elliptic (v_2) flows of free protons from ^{197}Au + ^{197}Au collisions at 40, 100, and 150 MeV/nucleon with different $\mathcal{F}$ is shown in Fig. 3. One can see that both v_1 and v_2 obtained with different $\mathcal{F}$ are different, and the differences become more evident with increasing beam energy. The reason is that with increasing beam energy, the collision term plays a more important role. The v_1 and v_2 values obtained with the FU3FP1 and $\mathcal{F} = 0.3$ are very close to each other. In addition, with a larger $\mathcal{F}$, which means a smaller reduction in the cross section, one can obtain a larger slope for v_1 and a more negative v_2 at mid-rapidity, $y_z/y_{\mathrm{pro}} = 0$. Nucleons are known to be more likely to undergo a bounce-off (positive v_1 slope) motion and

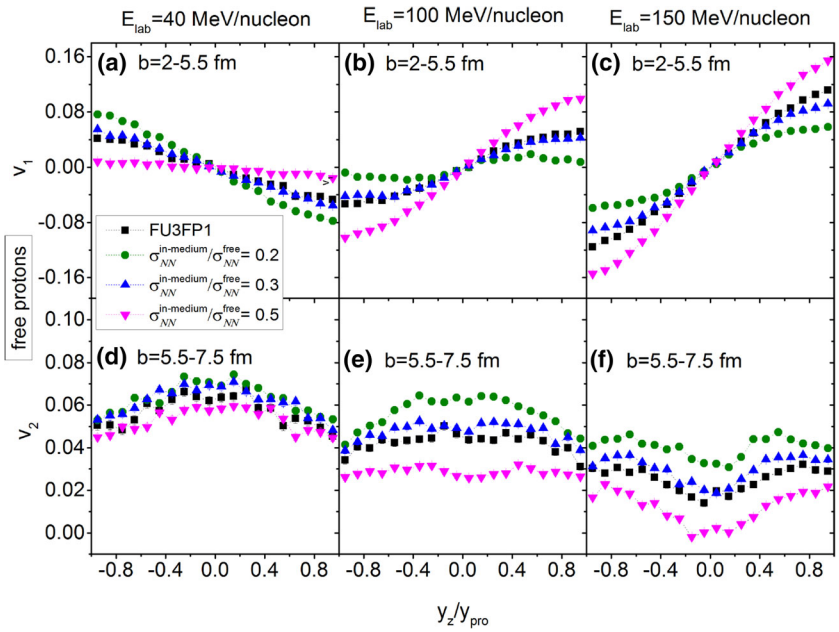

Fig. 3 (Color online) Rapidity distribution of the directed flow v_1 (upper, b = 2–5.5 fm) and elliptic flow v_2 (lower, b = 5.5–7.5 fm) of free protons from Au + Au collisions at $E_{\rm lab}$ = 40 (left panels), 100 (middle panels), and 150 MeV/nucleon (right panels)

squeeze-out (negative v_2) pattern because of the increasing collision number.

Figure 4 shows the v_1 slope and v_2 at $y_z/y_{\rm pro}$ = 0 for hydrogen isotopes calculated with different $\mathcal{F}$ values in comparison with the FOPI and INDRA experimental data. The chosen impact parameters are b = 2–5.5 fm and b = 5.5–7.5 fm for v_1 and v_2, respectively. The v_1 slope is obtained assuming $v_1(y_0) = v_{11}y_0 + v_{13}y_0^3 + c$ in the range of $|y_0| = |y_z/y_{\rm pro}| < 0.4$. With increasing $E_{\rm lab}$, the value of the v_1 slope increases and the value of v_2 decreases. The results obtained with FU3FP1 and $\mathcal{F} = 0.3$ are very close to each other. Furthermore, the correction factors $\mathcal{F}$ = 0.2 and 0.5 are required to fit the experimental data at beam energies of 40 and 150 MeV/nucleon, respectively. In addition, calculations with the FU3FP1 parametrization can simultaneously reproduce both v_1 and v_2 well.

To understand more clearly the influence of the medium correction factor on the NNCS, Fig. 5 shows the proton energy spectra of ^{197}Au + ^{197}Au collisions at beam energies of 40 and 150 MeV/nucleon. Overall, the energy spectra drop exponentially with energy and can also be affected by changing the medium correction factor. The energy spectrum obtained with $\mathcal{F} = \sigma_{\rm NN}^{\rm in-medium}/\sigma_{\rm NN}^{\rm free} = 0.2$ has a steeper slope than the others because the number of collisions is smallest in this case.

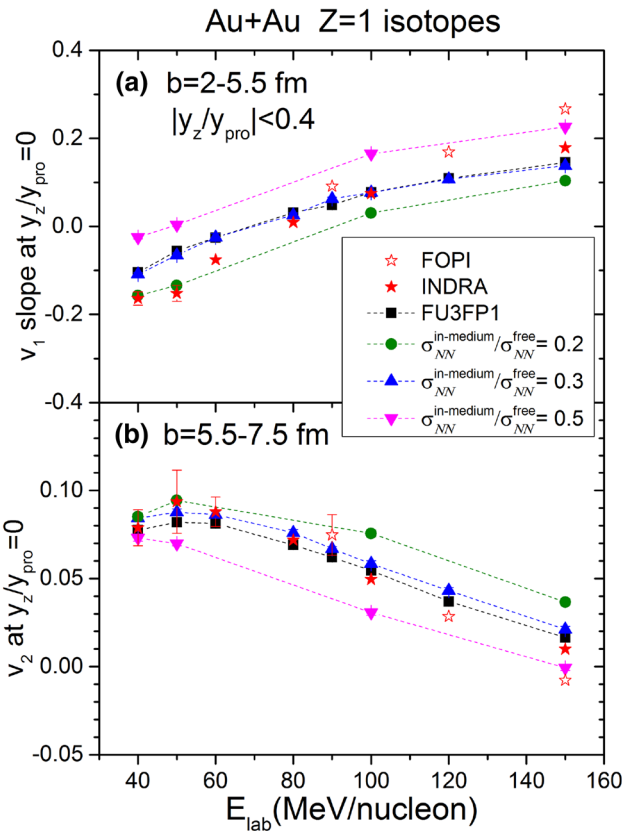

Fig. 4 (Color online) Flow excitation functions at mid-rapidity for hydrogen isotopes from ^{197}Au + ^{197}Au collisions. The results with four in-medium correction factors are represented by different symbols and lines as indicated. The FOPI experimental data (open stars) and INDRA experimental data (solid stars) are taken from Ref. [69]

3.3 Nuclear stopping

The nuclear stopping power is another important observable that characterizes the transparency of colliding nuclei [15, 19–21, 50]. In this work, we calculated the two quantities $R_{\rm E}$ and *vartl* for the same reaction. The former

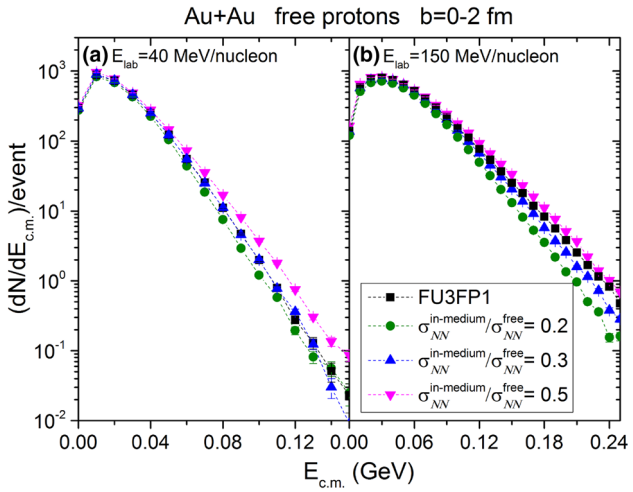

Fig. 5 (Color online) Kinetic energy distribution of free protons from ^{197}Au +^{197} Au central collisions at beam energies of 40 (left panels) and 150 (right panels) MeV/nucleon

was proposed by the FOPI collaboration [70] and is defined as the ratio of the variances of the transverse and longitudinal rapidity distributions:

$$vartl = \frac{\langle y_x^2 \rangle}{\langle y_z^2 \rangle}, \langle y_{x,z}^2 \rangle = \frac{\sum (y_{x,z}^2 N_{y_{x,z}})}{\sum N_{y_{x,z}}}. \quad (12)$$

The other quantity, R_{E}, was proposed by the INDRA collaboration and is defined as the ratio of the transverse and parallel energies:

$$R_{\mathrm{E}} = \frac{\sum E_{\perp}}{2 \sum E_{\parallel}}, \quad (13)$$

where $E_{\perp}$ ($E_{\parallel}$) is the transverse (parallel) kinetic energy of particles in the center-of-mass system [72].

The beam energy dependence of the degree of nuclear stopping for free protons in central HICs is displayed in Fig. 6. Similar to the results shown in Fig. 4, the degree of nuclear stopping can be reproduced well with $\mathcal{F} \approx 0.3$ at E_{lab} = 40 MeV/nucleon. However, $\mathcal{F} \approx 0.5$ is needed at E_{lab} = 150 MeV/nucleon. With increasing beam energy, a nuclear medium with higher density and momentum can be created; thus, it is reasonable that the reduction factors at different beam energies are different. With increasing beam energy, the difference in R_{E} between $\mathcal{F} = 0.3$ and FU3FP1 increases steadily. The experimental data and the trend in stopping power with increasing beam energy can be reproduced reasonably well by the calculations with FU3FP1. In contrast, the other calculations remain almost constant because the reduced factor in the FU3FP1 depends on both the density and momentum. In addition, these conclusions can be confirmed in both ^{197}Au +^{197} Au and ^{129}Xe +^{120} Sn.

4 Summary

The effects of the in-medium nucleon–nucleon cross section on the collective flow and nuclear stopping in the Fermi energy domain are investigated within the UrQMD model, in which medium correction factors of $\mathcal{F} = \sigma_{\mathrm{NN}}^{\mathrm{in-medium}}/\sigma_{\mathrm{NN}}^{\mathrm{free}} = 0.2, 0.3, 0.5$ and the parametrization factor FU3FP1 (which is density and momentum dependent) are considered. It is demonstrated that to best fit both the collective flow and nuclear stopping data, $\mathcal{F} \approx 0.2$ and 0.5 are required at beam energies of 40 and 150 MeV/

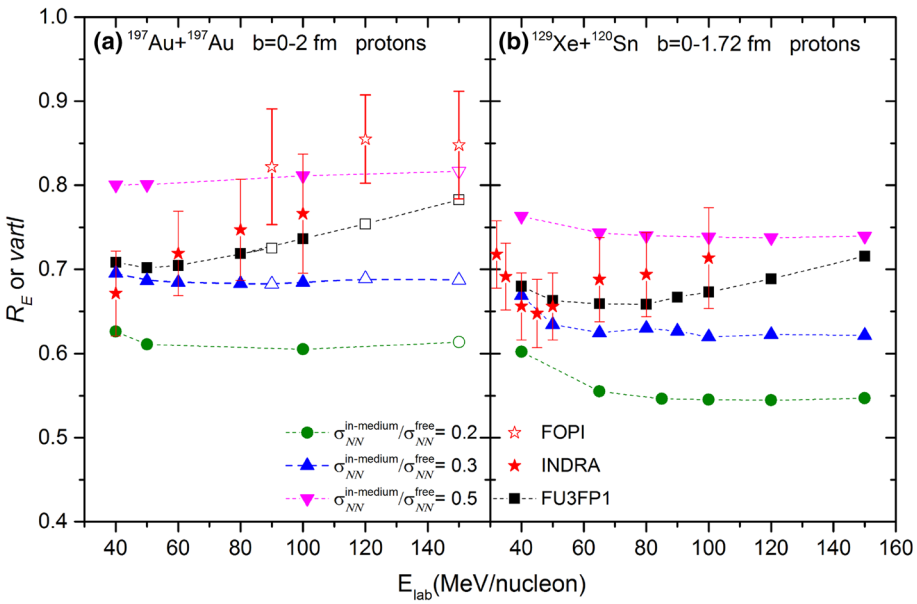

Fig. 6 (Color online) Comparison of R_{E} (solid symbols) and *vartl* (open symbols) for free protons from central ^{197}Au +^{197} Au (left panels) and ^{129}Xe +^{120} Sn (right panels) collisions with four different medium correction factors (dashed lines with different symbols) to the FOPI (open stars) and INDRA (solid stars) experimental data [42, 73]

nucleon, respectively. These results are consistent with the results obtained by the INDRA collaboration. The calculations with the FU3FP1 parametrization reproduce both the directed and elliptic flow data reasonably well. The slightly increased stopping power with increasing beam energy can also be found in the calculations with the FU3FP1 parametrization, whereas the calculations with $\mathcal{F}$ = 0.2, 0.3, and 0.5 yield roughly flat energy-dependent.

References

1. J. Aichelin, "Quantum" molecular dynamics—a dynamical microscopic n-body approach to investigate fragment formation and the nuclear equation of state in heavy ion collisions. Phys. Rep. **202**, 233 (1991). https://doi.org/10.1016/0370-1573(91)90094-3
2. G.F. Bertsch, S. Das Gupta, A guide to microscopic models for intermediate energy heavy ion collisions. Phys. Rep. **160**, 189 (1988). https://doi.org/10.1016/0370-1573(88)90170-6
3. J. Xu, L.W. Chen, M.B. Tsang et al., Understanding transport simulations of heavy-ion collisions at 100*A* and 400*A* MeV: comparison of heavy-ion transport codes under controlled conditions. Phys. Rev. C **93**, 044609 (2016). https://doi.org/10.1103/PhysRevC.93.044609
4. Y.X. Zhang, Y.J. Wang, M. Colonna et al., Comparison of heavy-ion transport simulations: collision integral in a box. Phys. Rev. C **97**, 034625 (2018). https://doi.org/10.1103/PhysRevC.97.034625
5. Z.F. Zhang, D.Q. Fang, Y.G. Ma, Decay modes of highly excited nuclei. Nucl. Sci. Tech. **29**, 78 (2018). https://doi.org/10.1007/s41365-018-0427-8
6. P. Danielewicz, R. Lacey, W.G. Lynch, Determination of the equation of state of dense matter. Science **298**, 1592 (2002). https://doi.org/10.1126/science.1078070
7. X.G. Deng, Y.G. Ma, Electromagnetic field effects on nucleon transverse momentum for heavy ion collisions around 100?*A*?MeV. Nucl. Sci. Tech. **28**, 182 (2017). https://doi.org/10.1007/s41365-017-0337-1
8. Y.J. Wang, C.C. Guo, Q.F. Li, A. Le Fèvre, Y. Leifels, W. Trautmann, Determination of the nuclear incompressibility from the rapidity-dependent elliptic flow in heavy-ion collisions at beam energies 0.4 A–1.0 A GeV. Phys. Lett. B **778**, 207 (2018). https://doi.org/10.1016/j.physletb.2018.01.035
9. H.M. Xu, Disappearance of flow and the in-medium nucleon–nucleon cross section. Phys. Rev. C **46**, R389 (1992). https://doi.org/10.1103/PhysRevC.46.R389
10. G.D. Westfall, W. Bauer, D. Craig et al., Mass dependence of the disappearance of flow in nuclear collisions. Phys. Rev. Lett. **71**, 1986 (1993). https://doi.org/10.1103/PhysRevLett.71.1986
11. B.A. Li, A.T. Sustich, Differential flow in heavy-ion collisions at balance energies. Phys. Rev. Lett. **82**, 5004 (1999). https://doi.org/10.1103/PhysRevLett.82.5004
12. D.J. Magestro, W. Bauer, G.D. Westfall, Isolation of the nuclear compressibility with the balance energy. Phys. Rev. C **62**, 041603 (2000). https://doi.org/10.1103/PhysRevC.62.041603
13. J.Y. Liu, W.J. Guo, S.J. Wang et al., Nuclear stopping as a probe for in-medium nucleon–nucleon cross sections in intermediate energy heavy ion collisions. Phys. Rev. Lett. **86**, 975 (2001). https://doi.org/10.1103/PhysRevLett.86.975
14. D. Persram, C. Gale, Elliptic flow in intermediate energy heavy ion collisions and in-medium effects. Phys. Rev. C **65**, 064611 (2002). https://doi.org/10.1103/PhysRevC.65.064611
15. T. Gaitanos, C. Fuchs, H.H. Wolter, Nuclear stopping and flow in heavy-ion collisions and the in-medium NN cross section. Phys. Lett. B **609**, 241 (2005). https://doi.org/10.1016/j.physletb.2005.01.069
16. B.A. Li, P. Danielewicz, W.G. Lynch, Probing the isospin dependence of the in-medium nucleon–nucleon cross sections with radioactive beams. Phys. Rev. C **71**, 054603 (2005). https://doi.org/10.1103/PhysRevC.71.054603
17. B.A. Li, L.W. Chen, Nucleon–nucleon cross sections in neutron-rich matter and isospin transport in heavy-ion reactions at intermediate energies. Phys. Rev. C **72**, 064611 (2005). https://doi.org/10.1103/PhysRevC.72.064611
18. Q.F. Li, Z.X. Li, S. Soff et al., Medium modifications of the nucleon–nucleon elastic cross section in neutron-rich intermediate energy HICs. J. Phys. G Nucl. Part. Phys. **32**, 407 (2006). https://doi.org/10.1088/0954-3899/32/4/001
19. Y.X. Zhang, Z.X. Li, Elliptic flow and system size dependence of transition energies at intermediate energies. Phys. Rev. C **74**, 014602 (2006). https://doi.org/10.1103/PhysRevC.74.014602
20. Y.X. Zhang, Z.X. Li, P. Danielewicz, In-medium NN cross sections determined from the nuclear stopping and collective flow in heavy-ion collisions at intermediate energies. Phys. Rev. C **75**, 034615 (2007). https://doi.org/10.1103/PhysRevC.75.034615
21. Y. Yuan, Q.F. Li, Z.X. Li et al., Transport model study of nuclear stopping in heavy-ion collisions over the energy range from 0.09*A* to 160*A* GeV. Phys. Rev. C **81**, 034913 (2010). https://doi.org/10.1103/PhysRevC.81.034913
22. G.Q. Zhang, Y.G. Ma, X.G. Cao et al., Unified description of nuclear stopping in central heavy-ion collisions from 10*A* MeV to 1.2*A* GeV. Phys. Rev. C **84**, 034612 (2011). https://doi.org/10.1103/PhysRevC.84.034612
23. D.D.S. Coupland, W.G. Lynch, M.B. Tsang et al., Influence of transport variables on isospin transport ratios. Phys. Rev. C **84**, 054603 (2011). https://doi.org/10.1103/PhysRevC.84.054603
24. Z.Q. Feng, Nuclear in-medium effects and collective flows in heavy-ion collisions at intermediate energies. Phys. Rev. C **85**, 014604 (2012). https://doi.org/10.1103/PhysRevC.85.014604
25. Y.X. Zhang, D.D.S. Coupland, P. Danielewicz et al., Influence of in-medium NN cross sections, symmetry potential, and impact parameter on isospin observables. Phys. Rev. C **85**, 024602 (2012). https://doi.org/10.1103/PhysRevC.85.024602
26. J. Su, ChY Huang, W.J. Xie et al., Effects of in-medium nucleon–nucleon cross sections on stopping observable and ratio of free protons in heavy-ion collisions at 400 MeV/nucleon. Eur. Phys. J. A **52**, 207 (2016). https://doi.org/10.1140/epja/i2016-16207-x
27. W.G. Love, M.A. Franey, Effective nucleon–nucleon interaction for scattering at intermediate energies. Phys. Rev. C **24**, 3 (1981). https://doi.org/10.1103/PhysRevC.24.1073
28. G.Q. Li, R. Machleidt, Microscopic calculation of in-medium nucleon–nucleon cross sections. Phys. Rev. C **48**, 1702 (1993). https://doi.org/10.1103/PhysRevC.48.1702
29. G.Q. Li, R. Machleidt, Microscopic calculation of in-medium proton–proton cross sections. Phys. Rev. C **49**, 566 (1994). https://doi.org/10.1103/PhysRevC.49.566
30. G.J. Mao, Z.X. Li, Y.Z. Zhuo et al., Medium effects on the NN inelastic cross section in relativistic heavy-ion collisions. Phys. Lett. B **327**, 183 (1994). https://doi.org/10.1016/0370-2693(94)90715-3
31. G.J. Mao, Z.X. Li, Y.Z. Zhuo et al., Study of in-medium NN inelastic cross section from relativistic Boltzmann–Uehling–Uhlenbeck approach. Phys. Rev. C **49**, 3137 (1994). https://doi.org/10.1103/PhysRevC.49.3137
32. T. Alm, G. Röpke, W. Bauer et al., The in-medium nucleon–nucleon cross section and BUU simulations of heavy-ion reactions. Nucl. Phys. A **587**, 815 (1995). https://doi.org/10.1016/0375-9474(95)00026-W

33. H.J. Schulze, A. Schnell, G. Ropke et al., Nucleon–nucleon cross sections in nuclear matter. Phys. Rev. C **55**, 3006 (1997). https://doi.org/10.1103/PhysRevC.55.3006
34. C. Fuchs, A. Faessler, M. El-Shabshiry, Off-shell behavior of the in-medium nucleon–nucleon cross section. Phys. Rev. C **64**, 024003 (2001). https://doi.org/10.1103/PhysRevC.64.024003
35. F. Sammarruca, P. Krastev, Effective nucleon–nucleon cross sections in symmetric and asymmetric nuclear matter. Phys. Rev. C **73**, 014001 (2006). https://doi.org/10.1103/PhysRevC.73.014001
36. H.F. Zhang, Z.H. Li, U. Lombardo et al., Nucleon–nucleon cross sections in dense nuclear matter. Phys. Rev. C **76**, 054001 (2007). https://doi.org/10.1103/PhysRevC.76.054001
37. H.F. Zhang, U. Lombardo, W. Zuo, Transport parameters in neutron stars from in-medium *NN* cross sections. Phys. Rev. C **82**, 015805 (2010). https://doi.org/10.1103/PhysRevC.82.015805
38. Q.F. Li, Z.X. Li, G.J. Mao, Isospin dependence of nucleon–nucleon elastic cross section. Phys. Rev. C **62**, 014606 (2000). https://doi.org/10.1103/PhysRevC.62.014606
39. Q.F. Li, Z.X. Li, E.G. Zhao, Density and temperature dependence of nucleon–nucleon elastic cross section. Phys. Rev. C **69**, 017601 (2004). https://doi.org/10.1103/PhysRevC.69.017601
40. Q.F. Li, Z.X. Li, The isospin dependent nucleon–nucleon inelastic cross section in the nuclear medium. Phys. Lett. B **773**, 557 (2017). https://doi.org/10.1016/j.physletb.2017.09.013
41. J. Chen, Z.Q. Feng, J.S. Wang, Nuclear in-medium effects on η dynamics in proton–nucleus collisions. Nucl. Sci. Tech. **27**, 73 (2016). https://doi.org/10.1007/s41365-016-0069-7
42. O. Lopez, D. Durand, G. Lehaut et al., (INDRA Collaboration), In-medium effects for nuclear matter in the Fermi-energy domain. Phys. Rev. C **90**, 064602 (2014). https://doi.org/10.1103/PhysRevC.90.064602
43. B. Rubina, K. Mandeep, K. Suneel, Correlation between directed transverse flow and nuclear stopping around the energy of vanishing flow. Indian J. Phys. **89**, 967 (2015). https://doi.org/10.1007/s12648-015-0672-1
44. Z. Basrak, P. Eudes, V. de la Mota, Aspects of the momentum dependence of the equation of state and of the residual NN cross section, and their effects on nuclear stopping. Phys. Rev. C **93**, 054609 (2016). https://doi.org/10.1103/PhysRevC.93.054609
45. H.L. Liu, Y.G. Ma, A. Bonasera et al., Mean free path and shear viscosity in central ^{129}Xe $+^{119}$ Sn collisions below 100 MeV/nucleon. Phys. Rev. C **96**, 064604 (2017). https://doi.org/10.1103/PhysRevC.96.064604
46. Y.Z. Xing, H.F. Zhang, X.B. Liu et al., Pauli-blocking effect in two-body collisions dominates the in-medium effects in heavy-ion reactions near Fermi energy. Nucl. Phys. A **957**, 135 (2017). https://doi.org/10.1016/j.nuclphysa.2016.08.006
47. Z.Q. Feng, Nuclear dynamics and particle production near threshold energies in heavy-ion collisions. Nucl. Sci. Tech. **29**, 40 (2018). https://doi.org/10.1007/s41365-018-0379-z
48. B.A. Li, B.J. Cai, L.W. Chen et al., Isospin dependence of nucleon effective masses in neutron-rich matter. Nucl. Sci. Tech. **27**, 141 (2016). https://doi.org/10.1007/s41365-016-0140-4
49. Q.F. Li, Z.X. Li, S. Soff et al., Probing the equation of state with pions. J. Phys. G **32**, 151 (2006). https://doi.org/10.1088/0954-3899/32/2/007
50. Q.F. Li, C.W. Shen, C.C. Guo et al., Nonequilibrium dynamics in heavy-ion collisions at low energies available at the GSI Schwerionen Synchrotron. Phys. Rev. C **83**, 044617 (2011). https://doi.org/10.1103/PhysRevC.83.044617
51. Y.J. Wang, C.C. Guo, Q.F. Li et al., Constraining the high-density nuclear symmetry energy with the transverse-momentum-dependent elliptic flow. Phys. Rev. C **89**, 044603 (2014). https://doi.org/10.1103/PhysRevC.89.044603
52. Y.J. Wang, C.C. Guo, Q.F. Li et al., Collective flow of light particles in Au + Au collisions at intermediate energies. Phys. Rev. C **89**, 034606 (2014). https://doi.org/10.1103/PhysRevC.89.034606
53. Y.J. Wang, C.C. Guo, Q.F. Li et al., Influence of differential elastic nucleon–nucleon cross section on stopping and collective flow in heavy-ion collisions at intermediate energies. Phys. Rev. C **94**, 024608 (2016). https://doi.org/10.1103/PhysRevC.94.024608
54. C. Hartnack, R.K. Puri, J. Aichelin et al., Modelling the many-body dynamics of heavy ion collisions: present status and future perspective. Eur. Phys. J. A **1**, 151 (1998). https://doi.org/10.1007/s100500050045
55. Y.J. Wang, C.C. Guo, Q.F. Li et al., 3H/3He ratio as a probe of the nuclear symmetry energy at sub-saturation densities. Eur. Phys. J. A **51**, 37 (2015). https://doi.org/10.1140/epja/i2015-15037-8
56. P.C. Li, Y.J. Wang, Q.F. Li, H.F. Zhang, Effects of the in-medium nucleon-nucleon cross section on collective flow and nuclear stopping in heavy-ion collisions in the Fermi-energy domain. Phys. Rev. C **97**, 044620 (2018). https://doi.org/10.1103/PhysRevC.97.044620
57. Q.F. Li, C.W. Shen, M. Di Toro, Probing the momentum-dependent medium modifications of the nucleon–nucleon elastic cross section. Mod. Phys. Lett. A **25**, 669 (2010). https://doi.org/10.1142/S0217732310032846
58. W.M. Guo, G.C. Yong, Y.J. Wang, Q.F. Li, H.F. Zhang, W. Zuo, Model dependence of isospin sensitive observables at high densities. Phys. Lett. B **726**, 211 (2013). https://doi.org/10.1016/j.physletb.2013.07.056
59. H. Kruse, B.V. Jacak, J.J. Molitoris et al., Vlasov–Uehling–Uhlenbeck theory of medium energy heavy ion reactions: role of mean field dynamics and two body collisions. Phys. Rev. C **31**, 1770 (1985). https://doi.org/10.1103/PhysRevC.31.1770
60. P. Russotto, P.Z. Wu, M. Zoric et al., Symmetry energy from elliptic flow in 197Au+197Au. Phys. Lett. B **697**, 471 (2011). https://doi.org/10.1016/j.physletb.2011.02.033
61. Q.F. Li, Y.J. Wang, X.B. Wang et al., Influence of coalescence parameters on the production of protons and Helium-3 fragments. Sci. China Phys. Mech. Astron. **59**, 672013 (2016). https://doi.org/10.1007/s11433-016-0120-3
62. Q.F. Li, Y.J. Wang, X.B. Wang et al., Rapidity distribution of protons from the potential version of UrQMD model and the traditional coalescence afterburner. Sci. China Phys. Mech. Astron. **59**, 622001 (2016). https://doi.org/10.1007/s11433-015-5768-2
63. Q.F. Li, Y.J. Wang, X.B. Wang et al., Helium-3 production from Pb+Pb collisions at SPS energies with the UrQMD model and the traditional coalescence afterburner. Sci. China Phys. Mech. Astron. **59**, 622001 (2016). https://doi.org/10.1007/s11433-015-5775-3
64. Y.X. Zhang, Z.X. Li, C.S. Zhou et al., Effect of isospin-dependent cluster recognition on the observables in heavy ion collisions. Phys. Rev. C **85**, 051602 (2012). https://doi.org/10.1103/PhysRevC.85.051602
65. S. Kumar, Y.G. Ma, Directed flow of isospin sensitive fragments within a modified clusterization algorithm in heavy-ion collisions. Nucl. Sci. Tech. **24**, 050509 (2013). https://doi.org/10.13538/j.1001-8042/nst.2013.05.009
66. T.T. Ding, C.W. Ma, An improved thermometer for intermediate-mass fragments. Nucl. Sci. Tech. **27**, 132 (2016). https://doi.org/10.1007/s41365-016-0142-2
67. C.W. Ma, C.Y. Qiao, T.T. Ding, Y.D. Song, Temperature of intermediate mass fragments in simulated 40Ca + 40Ca reactions around the Fermi energies by AMD model. Nucl. Sci. Tech. **27**, 111 (2016). https://doi.org/10.1007/s41365-016-0112-8

68. H.L. Lao, F.H. Liu et al., Kinetic freeze-out temperatures in central and peripheral collisions: which one is larger ? Nucl. Sci. Tech. **29**, 82 (2018). https://doi.org/10.1007/s41365-018-0425-x
69. A. Andronic, J. Lukasik, W. Reisdorf et al., Systematics of stopping and flow in Au+ Au collisions. Eur. Phys. J. A **30**, 31 (2006). https://doi.org/10.1140/epja/i2006-10101-2
70. W. Reisdorf et al., Systematics of azimuthal asymmetries in heavy ion collisions in the 1*A* GeV regime. Nucl. Phys. A **876**, 1 (2012). https://doi.org/10.1016/j.nuclphysa.2011.12.006
71. H.C. Song, Y. Zhou, K. Gajdošová, Collective flow and hydrodynamics in large and small systems at the LHC. Nucl. Sci. Tech. **28**, 99 (2017). https://doi.org/10.1007/s41365-017-0245-4
72. G. Lehaut et al., Study of nuclear stopping in central collisions at intermediate energies. Phys. Rev. Lett. **104**, 232701 (2010). https://doi.org/10.1103/PhysRevLett.104.232701
73. W. Reisdorf et al., (FOPI Collaborations), Systematics of central heavy ion collisions in the 1A GeV regime. Nucl. Phys. A **848**, 366 (2010). https://doi.org/10.1016/j.nuclphysa.2010.09.008